Environ Monit Assess (2021) 193: 497
https://doi.org/10.1007/s10661-021-09301-w

Optimization for synthesis of silver nanoparticles through response surface methodology using leaf extract of *Boswellia sacra* and its application in antimicrobial activity

Syed Najmul Hejaz Azmi · Bushra Mohammed Hamed Al-Jassasi · Hiba Mohammed Saif Al-Sawafi · Sahar Harib Gharib Al-Shukaili · Nafisur Rahman · Mohd Nasir

Received: 3 February 2021 / Accepted: 12 July 2021 / Published online: 20 July 2021

Abstract In the present work, leaf extract of *Boswellia sacra* was used as reductant for synthesis of silver nanoparticles (AgNPs). The variables such as volume of *Boswellia sacra* leaf extract (1%), volume of silver nitrate (1 mM), and temperature were optimized by response surface methodology via Box-Behnken design for the synthesis of AgNPs. Design-Expert software generated the optimum conditions for the highest yield of silver nanoparticles as 8 mL of 1 mM $AgNO_3$, 8 mL of 1% *Boswellia sacra* leaf extract, and temperature = 55 °C. The formed AgNPs were isolated and purified by centrifugation process using ethanol/ distilled water. AgNPs were characterized using FTIR, SEM, TEM, EDX, and XRD. AgNPs showed surface plasmon resonance absorption band at 422 nm. XRD pattern indicated the crystalline nature of the particles (diameter 11.17 to 37.50 nm) with face-centered cubic structure. SEM and TEM images highlighted the formation of spherical AgNPs. The energy dispersive spectroscopic spectrum confirmed the presence of elemental silver. The microbial activity of AgNPs was evaluated against bacteria and fungi. Synthesized AgNPs were very effective against Gram-positive *E. coli* bacterial strains and fungal strains (*Penicillium chrysogenum*).

Keywords *Boswellia sacra* leaf extract · Silver nanoparticles · Surface plasmon resonance spectroscopy · X-ray diffraction · Antimicrobial activity

S. N. H. Azmi (✉) · B. M. H. Al-Jassasi · H. M. S. Al-Sawafi · S. H. G. Al-Shukaili
University of Technology and Applied Sciences, Applied Sciences Department (Chemistry Section), Higher College of Technology Muscat, P. O. Box 74, Al-Khuwair 133, Sultanate of Oman
e-mail: syed-azmi@hct.edu.om

N. Rahman · M. Nasir
Department of Chemistry, Aligarh Muslim University, Uttar Pradesh, Aligarh 202002, India

Introduction

Nanotechnology is one of the most promising field of research which involves the synthesis and application of matter with nanoscale. Newly synthesized or improved nanoparticles are clusters of microscopic particles ranging from 1 to 100 nm which exhibit specific size, form, and distribution pattern with extraordinary properties differing from those present in bulk (Kostoff et al., 2007; Raveendran et al., 2006). Silver nanoparticles can absorb and scatter light as well as exhibit colors depending on the shape, size, and morphology. Synthesis of silver nanoparticles has drawn attention owing to their various applications in medicines, biology, physics, and chemistry (Song & Kim, 2009; Xu et al., 2020; Zhang et al., 2018). Silver nanoparticles are also known to have antimicrobial and antifungal properties. Various techniques such as physical,

chemical, and biological methods have been used for the synthesis of silver nanoparticles. In chemical methods (Alqadi et al., 2014; Chen et al., 2020; De Matteis et al., 2015; Gudikandula & Charya Maringanti, 2016; Gusrizal et al., 2017; Guzman et al., 2012; Martínez-Castañón et al., 2008; Pastoriza-Santos & Liz-Marzán, 2002; Quintero-Quiroz et al., 2019; Zhang et al., 2011), the silver ions were reduced by both inorganic and organic reducing agents. Some of the reactants and starting materials used in the chemical methods for the synthesis of AgNPs are environmentally toxic or potentially hazardous. Researchers have focused their attention in developing methods based on the concept of green chemistry for the synthesis of AgNPs to reduce or eliminate the use of toxic reagents (Ahmed et al., 2016; Rafique et al., 2017; Mousavi et al., 2018; Ahmad et al., 2019; Tarannum & Divya, 2019). The syntheses of silver nanoparticles have been reported with plant extracts of *Achillea millefolium* (Yousaf et al., 2020), *Salvia spinose* (Pirtarighat et al., 2019), *Lysiloma acapulcensis* (Garibo et al., 2020), and *Origanum vulgare* L (Shaik et al., 2018); leaf extracts of *Tragopogon collinus* (Seifipour et al., 2020), *Diospyros lotus* (Hamedi & Shojaosadati, 2019), *Aesculum hippocastanum* (Küp et al., 2020), and *Atropa acuminate* (Rajput et al., 2020); flower extracts of *Datura inoxia* (Gajendran et al., 2019), *Allium sativum* (Velsankar et al., 2020), *Caesalpinia pulcherrima* (Moteriya & Chanda, 2017), and *Malva sylvestris* (Esfanddarani et al., 2018); and fruit extract of *Phyllanthus emblica* (Masum et al., 2019), *Andean blackberry* (Kumar et al., 2017), *Lycium* barbarum (Dong et al., 2017), and *Garcinia indica* (Sangaonkar & Pawar, 2018). Greener syntheses of AgNPs provide advancement over other methods as they are simple, one step, cost-effective, environment-friendly, and relatively reproducible and often result in more stable materials. There are many species of *Boswellia* like *Boswellia serrata*, *Boswellia sacra*, *Boswellia carterii*, and *Boswellia frereana*, but *Boswellia sacra* is commonly available in Oman especially in Dhofar region (Al-Harrasi et al., 2018). *Boswellia sacra* comes under the family of Burseraceae. The plant parts such as gum resin, leaf, bark, and roots are being used as a cosmetic agent and as a traditional medicine to treat variety of ailments including dengue, malaria, jaundice, and immunomodulatory and antiviral activity (Al-Harrasi & Al-Saidi, 2008). Efforts have been made to synthesize gold nanoparticles using resin gum extract of *Boswellia sacra* (United States Patent, 2017). Published data confirmed that leaves and bark of *Boswellia sacra* contain β-boswellic acid, 3-*O*-acetyl-11-keto-β-boswellic acid, and acetyl-β-boswellic acid (Al-Harrasi & Al-Saidi, 2008; Al-Harrasi et al., 2018; Hamidpour et al., 2013) which could be used as reducing agents. Hence, the reducing property of the *Boswellia sacra* leaf extract was exploited and utilized for synthesis of silver nanoparticles using silver nitrate as precursor. As per the literature review on *Boswellia sacra*, it seems to be that until now the leaf extract of *Boswellia sacra* was not tested for synthesis of silver nanoparticles.

Response surface methodology (RSM) is a collection of mathematical and statistical tools which is applied for designing experiments and optimizing the response affected by different variables. RSM is useful in examining the interactive effect of process variables and in developing the mathematical model to accurately describe the process (Rahman & Nasir, 2020a, b; Rahman & Varshney, 2020). RSM was used to optimize the variables of *Trichoderma viride*-mediated nanosilver synthesis (Othman et al., 2017). The synthesis condition of silver nanoparticles with the seed extract of *Plantago major* was optimized using central composite design (Nikaeen et al., 2020). The green synthesis of silver nanoparticles was performed with leaf extract of purple heart plant, and the independent variables such as silver nitrate concentration, temperature, and volume of leaf extract were optimized using Box-Behnken design (Hasnain et al., 2019).

In the present work, synthesis of silver nanoparticles was performed using aqueous leaf extract of *Boswellia sacra*. An attempt has been made to optimize the variables of synthesis process such as volumes of 1 mM silver nitrate and aqueous leaf extract of *Boswellia sacra* and temperature using RSM via Box-Behnken design. Under the optimized conditions, silver nanoparticles were synthesized, purified, and isolated. The characterization of silver nanoparticles was achieved by UV–visible spectrophotometry, FTIR, scanning electron microscopy, energy dispersive X-ray spectrometry, transmission electron microscopy, and X-ray diffraction. The antibacterial and antifungal activities of the synthesized silver nanoparticles were evaluated.

Experimental

Materials

The absorbance and spectra of leaf extract, silver nitrate, and silver nanoparticles solutions were recorded using UV–Vis spectrophotometer (Evolution 300-Thermo Fisher Scientific). The water bath thermostat (SBS40-

Stuart, UK) was used to maintain the temperature of the solutions. Dry *Boswellia sacra* leaves were blended using a blender (Preethi TRIO, India). Sixty mesh sieve was used to filter blended leaf powder of *Boswellia sacra*. Centrifuge (centrifuge 5810 R) machine was used to isolate and purify silver nanoparticles. FTIR spectra were obtained on an IR Affinity-1 Shimadzu spectrophotometer (Kyoto, Japan). Branson 2800 series ultrasonic sonicator (USA) was used to sonicate the powdered *Boswellia sacra* leaf. The instrumental facilities (on payment basis) of the Central Analytical and Applied Research Unit, Sultan Qaboos University, Oman, such as scanning electron microscope (SEM) (JSM 7600F, JEOL, Japan), attached with energy dispersive X-ray spectrometer (EDS) and X-ray diffractometer (XRD) (PANalytical, Xpert PRO, USA) with Ni filter using CuKα radiation (λ = 1.5418 Å) at 45 kV and 40 mA, and the DARIS, Centre for Scientific Research and Technological Development, Nizwa University, such as transmission electron microscope (TEM) (JEM-1400-JEOL, Japan), were utilized to characterize silver nanoparticles. OriginPro 2020b software (USA) was used to draw spectral graphs.

All reagents and solvents are of high-quality and analytical reagent grade. Silver nitrate was procured from Sigma-Aldrich, Germany, and 1 mM $AgNO_3$ solution was prepared in deionized water.

Bacteria such as *Escherichia coli* (ATCC 25,922) and *Staphylococcus aureus* (ATCC 25,932) and fungus such as *Penicillium chrysogenum* and *Rhizopus oryzae* were taken for antimicrobial activities. Agar and potato dextrose agar were purchased from HiMedia, India. Dimethyl sulfoxide (Merck, Germany) was used to dissolve materials for antimicrobial activities.

Methods

Preparation of fine powder of Boswellia sacra

Boswellia sacra leaves were collected from Al-Rustaq, Al-Batinah governorate, Oman. Professor Kesaraju Seeta Ram Chander Rao (a certified botanical surveyor) from the University of Technology & Applied Sciences, Higher College of Technology Muscat, Applied Biology, Applied Sciences Department, identified the plant as *Boswellia sacra*. The leaves were thoroughly rinsed with tap water and then with deionized water. The leaves were air dried for 2 days in a big stainless-steel sieve. The dried leaves (67 g) were blended using blender and sieved using 60 mesh sieve. The filtered leaf powder of *Boswellia sacra* was transferred into amber bottle and kept in dark to prevent decomposition of the material.

UV–visible spectra of Boswellia sacra leaf extract and silver nitrate

Boswellia sacra leaf extract (1%) was prepared by dissolving 0.5 g powdered *Boswellia sacra* leaf in 50 mL double distilled water with (a) manual stirring at room temperature, (b) stirring for 5 min at 300 rpm on a linear shaker at room temperature, and (c) heating at 40 °C. The solutions were filtered, separately, using suction filtration. The filtrates were transferred into 50-mL volumetric flasks and made up to volume with double deionized water. One milliliter of each extract (1%) was diluted to 25 mL with deionized water, and the absorption spectrum was recorded in the range of 190–340 nm. The aqueous leaf extract was utilized for synthesis of silver nanoparticles.

One milliliter of 1 mM $AgNO_3$ was diluted to 25 mL deionized water, and its absorption spectrum was recorded in the wavelength range of 190–340 nm.

Box-Behnken design for optimization

RSM with Box-Behnken design has been applied to optimize the synthesis parameters of silver nanoparticles with regard to high yield. This study focuses the effects of three variables such as volume of 1 mM $AgNO_3$ (4–12 mL), volume of 1% *Boswellia sacra* extract (4–12 mL), and temperature (35–75 °C) on the yield of silver nanoparticles as absorbance at 422 nm. Each variable was considered at three levels (−1, 0, and + 1). Table 1 shows the ranges and levels of each factor. BBD matrix comprising of 17 trials (involving three variables, each variable at three levels) was obtained using Design-Expert software (trial version). Therefore, 17 experiments involving different combinations of 1 mM $AgNO_3$, 1% *Boswellia sacra* extract, and temperature were conducted according to the BBD matrix and response (absorbance at 422 nm) was recorded. Second-order polynomial equation was used to fit the experimental results (Azmi et al., 2020; Rahman et al., 2019):

$$Y = \beta_0 + \sum_{i=1}^{n} \beta_i X_i + \sum_{i=1}^{n} \beta_{ii} X_{i\,i}^2 + \sum_{i=1}^{n} \sum_{j>1}^{n} \beta_{ij} X_i X_j + \varepsilon \quad (1)$$

where Y is the predicted response; β_0 is the regression coefficient; and β_i, β_{ii}, and β_{ij} represent the linear,

Table 1 Ranges and levels of variables used in the Box-Behnken design

Variables	Unit	Factors	Range and levels		
			Low (−1)	Medium(0)	High (+1)
Volume of 1 mM $AgNO_3$	mL	A	4.00	8.00	12.00
Volume of 1% *Boswellia sacra* leaf extract	mL	B	4.00	8.00	12.00
Temperature	°C	C	35.00	55.00	75.00

quadratic, and interaction coefficients, respectively. X_i and X_j denote the coded levels of independent variables. ε is the random error. The analysis of variance (ANOVA) was performed to analyze the significance of model terms and their interactions.

Synthesis and purification of silver nanoparticles

Kimling and coworkers described the methodology for synthesis of gold nanoparticles (Kimling et al., 2006). The same methodology was adopted here for synthesis of silver nanoparticles. AgNPs were synthesized under the optimized conditions obtained by RSM. Forty milliliter of 1 mM $AgNO_3$ was pipetted into two conical flasks (250 mL) separately. To each flask, 40 mL of 1% *Boswellia sacra* leaves extract (burette) was added dropwise with stirring using Teflon-coated magnetic bar for 30 min at 55 ± 1 °C. The bath thermostat was used to maintain the temperature. The progress of the reaction was monitored by measuring the absorbance at 422 nm. The maximum absorbance was achieved with 40 mL of 1% *Boswellia sacra* leaves extract. The reaction mixture (conical flask 1) was transferred into 250-mL volumetric flask and diluted up to mark with deionized water. The mixture was kept in dark for 1 day. The reaction mixture (conical flask 2) was transferred into a 500-mL beaker and covered with aluminum sheet. The resulting mixture was kept in refrigerator at – 5 °C for 1 day. The lower temperature leads to the better growth of AgNPs (Riaz et al., 2021). Finally, the dark brown silver nanoparticles were formed. The supernatant liquid was decanted, and the synthesized nanoparticles were taken in double distilled water. The nanoparticles in distilled water were transferred into centrifugation tube and centrifuged at 12,000 round per minute for 5 min. The silver nanoparticles were recovered, and distilled water was added again. Again, the synthesized silver nanoparticles were transferred into centrifugation tube and centrifuged for 5 min at 12,000 rpm. The silver nanoparticles were recovered and followed the same centrifugation process. Later on, the same recovered silver nanoparticles were cleaned with ethanol at least 3 times. Finally, the silver nanoparticles were isolated into cleaned crucible and kept in an oven at 110 °C for 30 min to dry the silver nanoparticles. After drying, the silver nanoparticles were transferred into sample tube and used for characterization and applications.

Characterization of silver nanoparticles

Silver nanoparticles were characterized by UV–visible spectrometry, FTIR spectroscopy, XRD, SEM, EDX, and TEM.

Antimicrobial activities

One percent (10 mg mL^{-1}) of test solutions of silver nanoparticles, *Boswellia sacra* leaf extract, silver nitrate, ampicillin (control for antibacterial activity), and nystatin (control for antifungal activity) were prepared by dissolving 0.1 g of said materials in 10 mL dimethyl sulfoxide and sonicated at 30 °C for 15 min. The test microorganisms such as *Escherichia coli* and *Staphylococcus aureus* were collected from University of Technology and Applied Sciences, Higher College of Technology Muscat, Microbiology Laboratory, as pure stock cultures. The inoculum was prepared. The pure colonies of bacteria were transferred from the mother stock plates with a sterile loop into the broth and incubated at 36 ± 1 °C in incubator shaker for 1 day. A paper disk dipped with test solutions in triplicate was placed in media containing *Escherichia coli* and *Staphylococcus aureus*. The plates were incubated at 36 ± 1 °C in incubator shaker for 1 day, and the zone of inhibition was measured in mm (diameter) and compared to determine the significance of AgNP as antibacterial agent.

For antifungal activities, petri plates containing potato dextrose agar were used to culture fungus

strains, namely *Penicillium chrysogenum* and *Rhizopus oryzae*. These plates were incubated at room temperature in incubator shaker for 3 days. A paper disk dipped in former 3 test solutions in triplicate was placed in media containing the selected fungus. These plates were placed in dark for 3 days at room temperature. The zone of inhibition was measured and compared with controlled (nystatin) inhibitory zone of inhibition to determine the significance of AgNP as antifungal agent. The experiments were repeated three times, and the mean value of zone of inhibition was calculated.

Results and discussion

The UV–visible spectrum of aqueous silver nitrate (colorless) was scanned, and a peak at 198 nm was observed (Fig. 1). The aqueous leaf extract of *Boswellia sacra* (1% w/v) is light yellow. The extraction of the compounds was investigated at room temperature with manual stirring, stirring at 300 rpm on linear shaker and at 40 °C. The UV–visible spectra of aqueous *Boswellia sacra* leaf extract in described conditions are scanned and shown in Fig. 1. It is evident from the Fig. 1 that the maximum absorbances of 1.585 and 0.43 were obtained at λ_{max} of 206 nm and 270 nm, respectively, with 1% aqueous *Boswellia sacra* leaf extract (leaf powder extracted at room temperature with 5 min of stirring at 300 rpm on linear shaker) and remained approximately same (maximum absorbance of 1.58 and 0.428 at λ_{max} of 206 nm and 270 nm, respectively) at 40 °C with 5 min of stirring at 300 rpm on linear shaker. Hence, the maximum extraction of the compounds of *Boswellia sacra* leaf was achieved with 5 min of stirring at 300 rpm on linear shaker at room temperature and hence could be employed for the synthesis of silver nanoparticles.

Box-Behnken design for optimization

The experiments were conducted to synthesize the silver nanoparticles according to BBD matrix, and the yield was measured in terms of absorbance at 422 nm. The results (Table 2) were subjected to multi-regression analysis using linear, 2-factor interaction and quadratic models. The statistical parameters are summarized in Table 3. The quadratic polynomial model showed highest values of F- and R^2 and lowest values of standard deviation, p- and PRESS. Therefore, quadratic model presented the dependence of high yield of silver nanoparticles synthesis on the volumes of 1 mM $AgNO_3$ and 1% *Boswellia sacra* extract and temperature. The quadratic regression model that correlates the response (absorbance at 422 nm) to the three selected variables in the synthesis of silver nanoparticles can be written as:

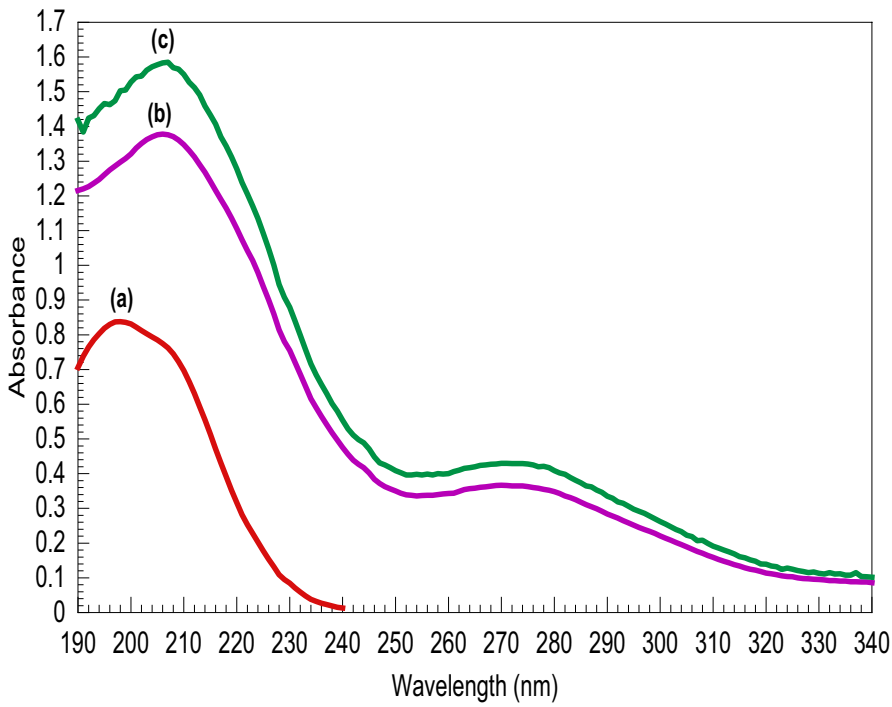

Fig. 1 UV–visible spectra: (**a**) 1 mM $AgNO_3$, (**b**) 1% *Boswellia sacra* leaf extract (manually shaking at RT for 5 min), (**c**) 1% *Boswellia sacra* leaf extract with 5-min shaking at 300 rpm on linear shaker at RT. In all cases, 1 mL aliquot was taken in 25 mL double distilled water

Table 2 Box-Behnken design matrix with experimental and predicted responses

Run	A	B	C	Actual (absorbance)	Predicted (absorbance)
1	8	8	55	1.309	1.309
2	8	4	75	0.693	0.695
3	4	8	35	0.398	0.399
4	4	12	55	0.787	0.787
5	8	8	55	1.309	1.309
6	12	8	35	0.424	0.422
7	4	8	75	0.699	0.701
8	8	12	75	1.16	1.16
9	8	12	35	0.383	0.381
10	4	4	55	0.803	0.7993
11	8	8	55	1.309	1.309
12	12	12	55	1.309	1.309
13	8	8	55	1.309	1.309
14	12	4	55	0.822	0.821
15	8	4	35	0.361	0.363
16	8	8	55	1.309	1.309
17	12	8	75	1.232	1.231

$$\text{Absorbance (yield)} = +1.31 + 0.1374\,A + 0.1200\,B + 0.2769\,C + 0.1258\,AB + 0.1261\,AC + 0.1111\,BC - 0.1704\,A^2 - 0.2088\,B^2 - 0.4516\,C^2 \quad (2)$$

The adequacy of the quadratic model in predicting the highest yield of silver nanoparticles was checked by ANOVA. The results of ANOVA are presented in Table 4. The model F- and *p*-values were 27,510.12 and < 0.0001, respectively, which suggested that the model is significant. Model terms with *p*-value less than 0.05 are said to be significant. Here, the linear terms (A, B, and C), interaction terms (AB, AC, and BC), and quadratic terms (A^2, B^2, and C^2) have *p*-values less than 0.05 which illustrated the statistical significance of model terms. Moreover, the adjusted R^2 is equal to predicted R^2 (0.9999) and, hence, is in ideal agreement for quadratic model. This demonstrated that the quadratic polynomial model explains well the correlation between the variables of synthesis of silver nanoparticles and the response. Additionally, R^2 value of 0.9998 indicated that 99.98% of the total variation on the synthesis data can be satisfactorily explained by the model and that only 0.02% variation cannot be described by the proposed model. The value of standard deviation (0.6231) suggested the reproducibility of the model.

The plot of actual response (measured absorbance at 422 nm) versus predicted response is shown in Fig. 2. It was observed that the data points are lying on the straight line because the average difference between the actual and predicted response is less than 0.01. It is concluded that the proposed quadratic model is appropriate and effective for optimization of process variables of synthesis of silver nanoparticles.

3D response surface plots

The regression equation is graphically represented as 3D response surface plots (Fig. 3). Figure 3a shows the combined effect of volumes of 1 mM $AgNO_3$ and 1% *Boswellia sacra* extract on the absorbance at 422 nm while keeping the temperature at the center level. It was observed that increasing the volumes of both $AgNO_3$ and *Boswellia sacra* extract resulted in increase in absorbance value, and the maximum absorbance (1.309) was obtained with 8 mL of each reagent. This indicated that the highest yield of silver nanoparticles was obtained on mixing equal volumes of 1 mM $AgNO_3$ and 1% *Boswellia sacra* extract. The interactive effect of volume of 1 mM $AgNO_3$ and temperature on the absorbance while keeping the volume of *Boswellia sacra* extract at its center level is shown in Fig. 3b. The highest yield was observed at 55 °C, and further increase in temperature caused a decrease in the yield. The combined effect of the volume of 1% *Boswellia sacra* extract and temperature on the absorbance, keeping the volume of $AgNO_3$ at its center level (Fig. 3c), revealed that the maximum absorbance was achieved with 8 mL of *Boswellia sacra* extract at 55 °C. Based on these observations, Design-Expert software generated the optimum conditions for the highest yield of silver nanoparticles which are given as volume of 1 mM $AgNO_3$ = 8 mL; volume of

Table 3 Statistical parameters of the polynomial models

Model	Std. Dev	F	*P* values	R^2	Adjusted R^2	Predicted R^2	PRESS	
Linear	13.2301	2.620	0.0953	0.3765	0.2326	0.0041	11,523.26	
2-factor interaction	11.3621	0.4677	0.7113	0.4532	0.1251	−0.5235	15,739.72	
Quadratic	0.6231	1091.400	< 0.0001	0.9998	0.9999	0.9999	19.73	Suggested

Table 4 Analysis of variance (ANOVA) for quadratic model

Sources	Sum of squares	df	Mean square	*F*-value	*p*-value	Remark
Model	2.32	9	0.2582	27,510.12	< 0.0001	Significant
A, volume of 1 mM AgNO3	0.1510	1	0.1510	16,089.04	< 0.0001	
B, volume of 1% *Boswellia sacra* leaf extract	0.1152	1	0.1152	12,266.99	< 0.0001	
C, temperature	0.6132	1	0.6132	65,319.92	< 0.0001	
AB	0.0633	1	0.0633	6746.22	< 0.0001	
AC	0.0636	1	0.0636	6773.05	< 0.0001	
BC	0.0494	1	0.0494	5261.99	< 0.0001	
A^2	0.1222	1	0.1222	13,018.20	< 0.0001	
B^2	0.1836	1	0.1836	19,557.62	< 0.0001	
C^2	0.8586	1	0.8586	91,461.58	< 0.0001	
Residual	0.0001	7	9.387E-06			
Lack of fit	0.0001	3	0.0000			
Pure error	0.0000	4	0.0000			
Cor total	2.32	16				

1% *Boswellia sacra* leaf extract = 8 mL, and temperature = 55 °C. The synthesis of silver nanoparticles was executed under the optimized experimental conditions in triplicate and resulted in an intense surface plasmon resonance absorption band at 422 nm (Fig. 4).

Characterization

The formation of silver nanoparticles was evidenced by the change in color from colorless silver ions to brown silver nanoparticles and showed as intense

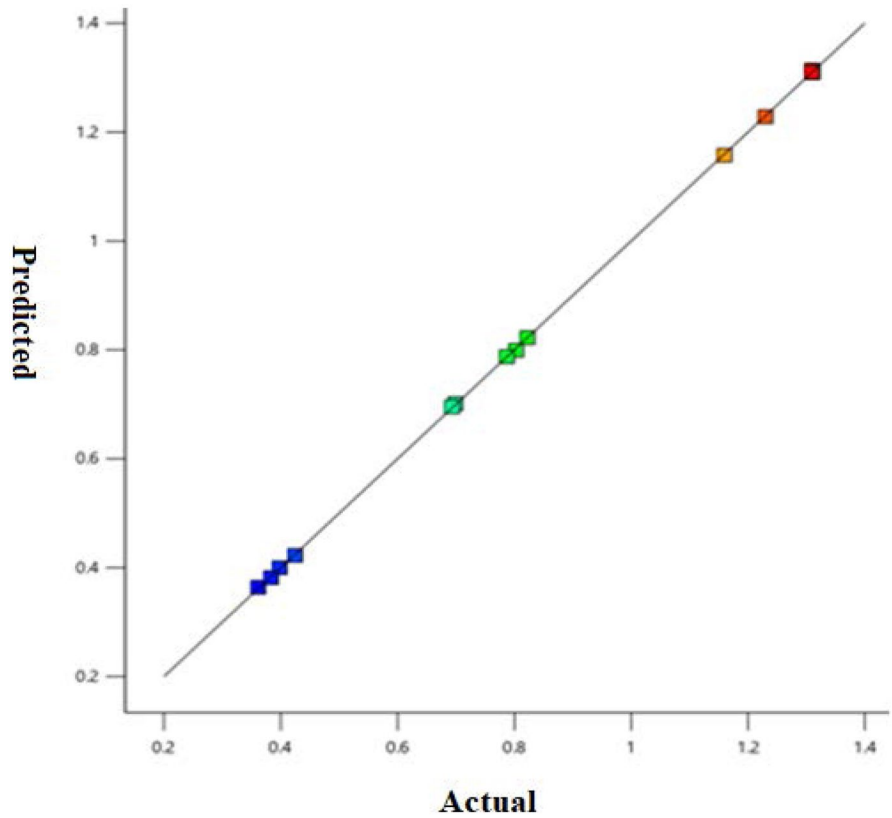

Fig. 2 Plot of measured response versus predicted responses

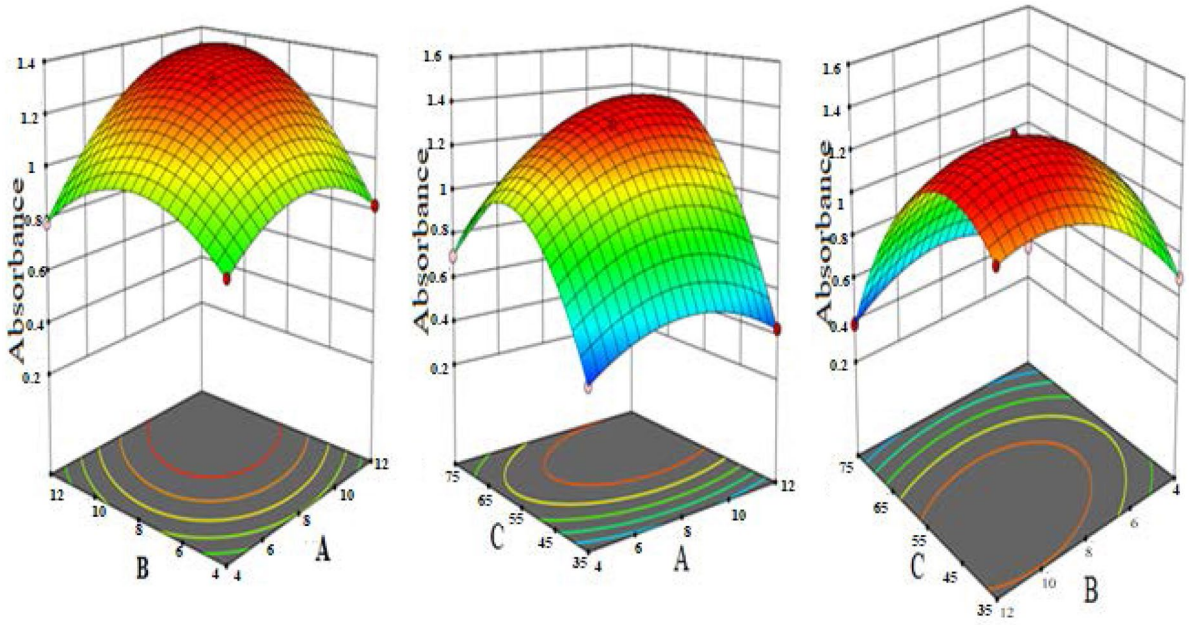

Fig. 3 3D response surface plots showing the effects of $AgNO_3$, *Boswellia sacra* leaf extract, and temperature on the synthesis of AgNPs by absorbance. Three pairs of parameters were optimized keeping the other parameter constant at a central point (zero level): (**a**) volumes of 1 mM $AgNO_3$ and 1% *Boswellia sacra* leaf extract, temperature at central point (**b**) volumes of 1 mM $AgNO_3$ and temperature, *Boswellia sacra* extract at central point and (**c**) volume of 1% *Boswellia sacra* leaf extract and temperature, silver nitrate solution at central point

surface plasmon resonance absorption band from 422 to 430 nm based on different sizes of silver nanoparticles (11.17 to 37.50 nm). The surface plasmon resonance absorption band at 422 nm was due to the stimulation of free electrons in the outermost orbitals of silver nanoparticles. It has been reported

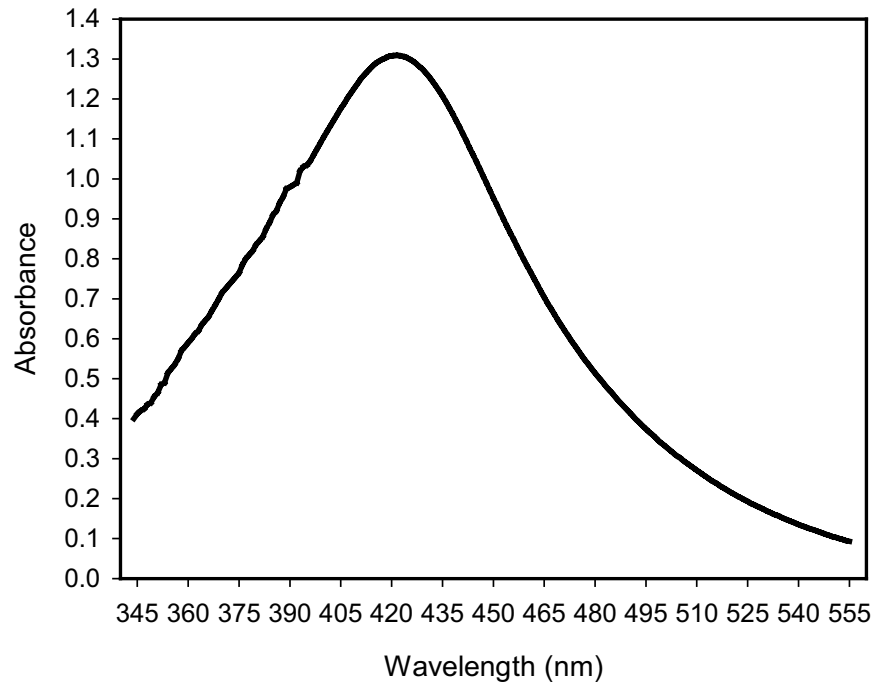

Fig. 4 Surface plasmon resonance absorption band of silver nanoparticles absorbed maximally at 422 nm (8 mL of 1% *Boswellia sacra* leaf extract + 8 mL of 1 mM $AgNO_3$ in 50-mL standard volumetric flask and diluted up to mark with distilled water at 55 ± 1 °C)

in the literature that spheroidal silver nanoparticles have plasmon absorption bands in the range of 400–500 nm (Sun et al., 2003). Hence, the synthesized silver nanoparticles are spherical in nature.

FTIR spectra of *Boswellia sacra* leaf extract (before reaction with $AgNO_3$) and AgNPs synthesized from leaf extract after reaction with $AgNO_3$ are presented in Fig. 5a, b. FTIR spectrum of *Boswellia sacra* leaf extract showed absorption bands at 3447.10, 2930.60, 1716.38, 1656.50, 1458.43, 1379.10, 1244.19, 1172.45, 1035.11, 891.13, 725.45, 613.66, and 441.56 cm^{-1}. FTIR spectrum of synthesized AgNPs revealed that the absorption band appearing at 3447.10 cm^{-1} was shifted to a lower wavenumber at 3422.10 cm^{-1} which indicated the binding of Ag^+ ion with hydroxyl or amine groups present in the leaf extract (Masum et al., 2019). The absorption band at 2930.60 cm^{-1} in both the spectra characterized the C-H stretching vibrations of methyl, methylene, or methoxy groups (Kathiravan et al., 2014). The absorption bands (Fig. 5) centered at 1716.38, 1656.50, and

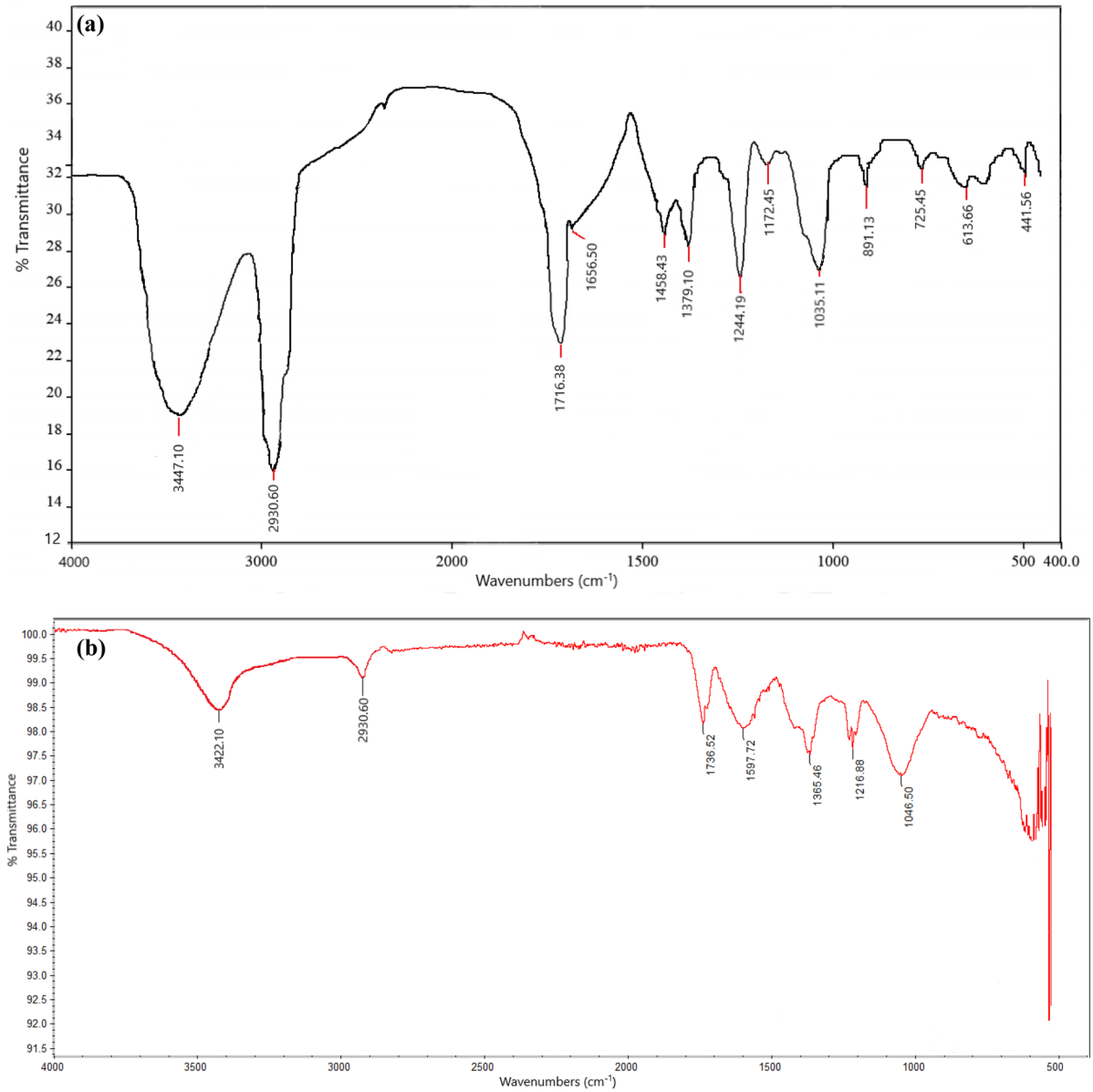

Fig. 5 FTIR spectra of (**a**) powdered leaf *Boswellia sacra* and (**b**) biosynthesized AgNPs

1035.11 cm^{-1} characterized the stretching vibrations of C=O (carboxylic acid) and C=O coupled to the amide linkage of proteins and C-N amine bond, respectively (Gole et al., 2001). On the other hand, the shift in band positions from 1716.38 to 1736.52 cm^{-1} and 1656.50 to 1597.72 cm^{-1} was observed in the FTIR spectrum of synthesized AgNPs which suggested the binding of C=O functional groups with AgNPs. Moreover, the absorption band peaking at 1458.43 cm^{-1} (Fig. 5a) indicated the stretching vibration of N–H present in the amide linkage of proteins, while this band was not observed in the FTIR spectrum of synthesized AgNPs (Fig. 5b), indicating the involvement of amide group in the capping and stabilization of AgNPs (Jyoti et al., 2016).

The X-ray diffraction spectra of the synthesized silver nanoparticles are shown in Fig. 6, which confirmed the crystalline property of the material. The silver peaks at 2θ (38.1342°, 44.4165°, 64.5248°, 77.4909°, and 81.6267°) and angle at full width at half maximum (0.2342, 0.8029, 0.3346, 0.4015, and 0.8029) using CuKα radiation (λ=0.15418 nm) were recorded. It is evident from the results of Fig. 6 that five 2θ values of 38.1342°, 44.4165°, 64.5248°, 77.4909°, and 81.6267° corresponding to hkl (111), (200), (220), (311), and (222) planes of silver are very much comparable to the standard X-ray diffraction powder patterns of silver (National Bureau of Standards Monograph, 1985). Hence, it is proved that the synthesized particles are silver with face-centered cubic symmetry. The crystallite size of silver nanoparticles was calculated using the following Scherrer's equation:

$$DP = k\lambda/\beta Cos\theta \tag{3}$$

where DP is crystallite size in nm, k is a constant (0.94), β is full width at half maximum in radians, θ *is* the diffraction angle, and λ is the wavelength of X-ray (0.15418 nm).

The crystallite size of synthesized silver nanoparticles was calculated and found to be 37.50, 11.17, 29.34, 26.51, and 13.66 nm.

The SEM images (magnification levels: 33,000 and 65,000) highlighted the formation of relatively

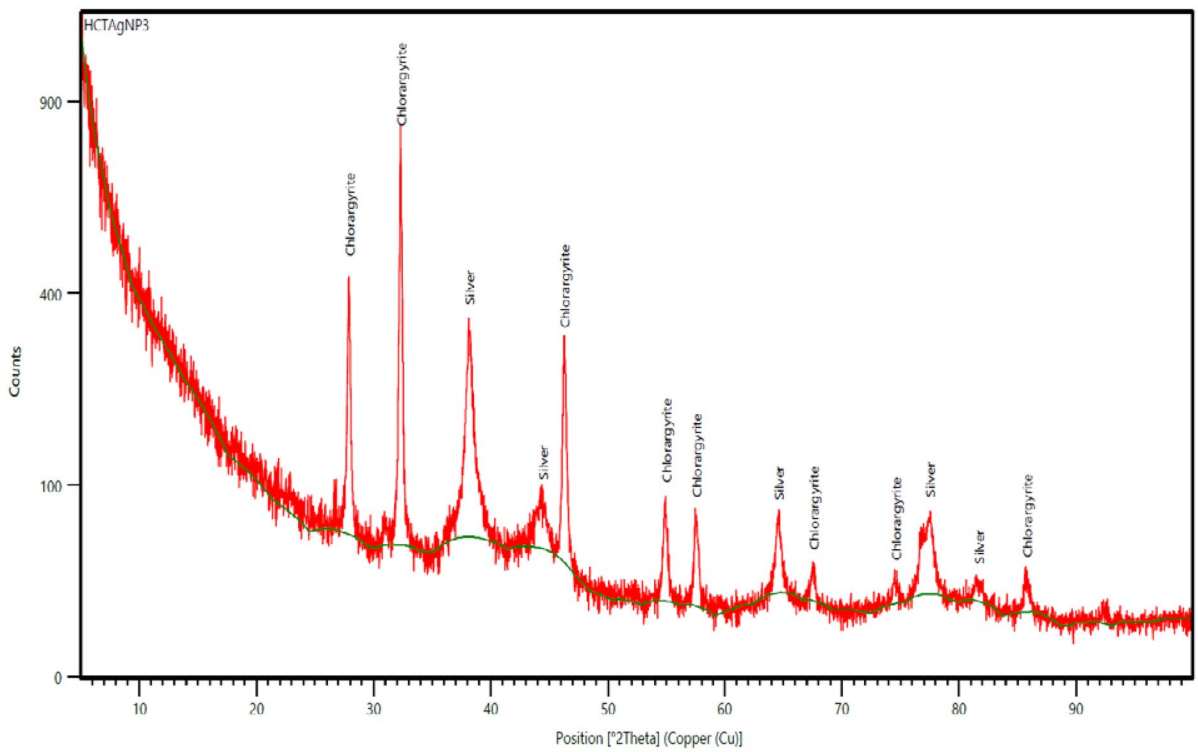

Fig. 6 XRD pattern of synthesized silver nanoparticles using extract of *Boswellia sacra* leaf

spherical and uniformly distributed silver nanoparticles within the bulk (Fig. 7). The size of AgNPs was in the range of 11.17–37.50 nm. Most of the AgNPs were aggregated, and some individual nanoparticles were also present. Similar observations were also reported for AgNPs prepared from *Tectona grandis* seeds extract (Rautela et al., 2019). The AgNPs in aggregate were not in direct contact which indicated the stabilization of nanoparticles by bioorganic capping molecules (Preetha et al., 2013).

The silver nanoparticles were analyzed by energy dispersive spectroscopy (Fig. 8). The energy dispersive spectroscopic spectrum confirmed the presence of elemental silver.

The TEM images of AgNPs showed that particles are spherical shaped in the range of 11.17

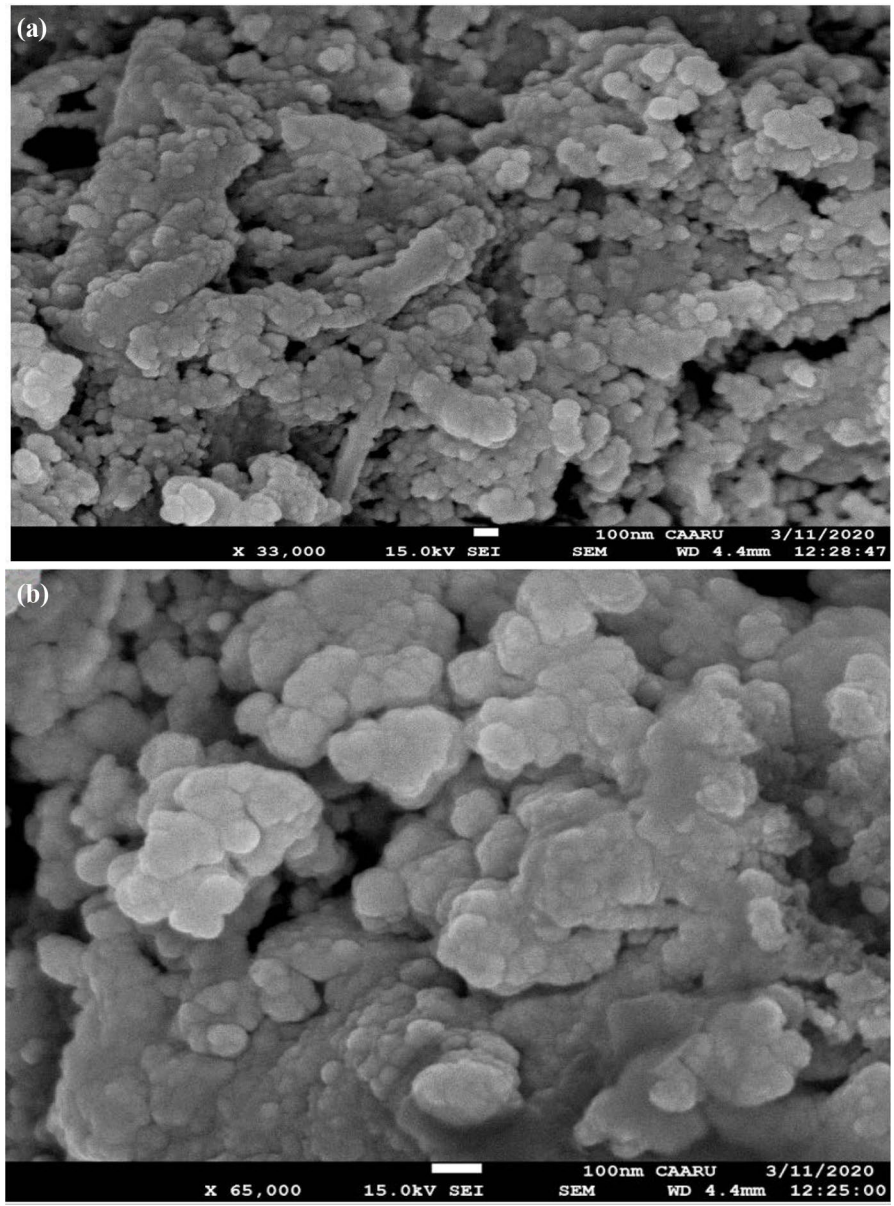

Fig. 7 SEM images of biosynthesized AgNPs (diameter size range: 11.17–37.50 nm) at different magnification levels (**a**) × 33,000 and (**b**) × 65,000

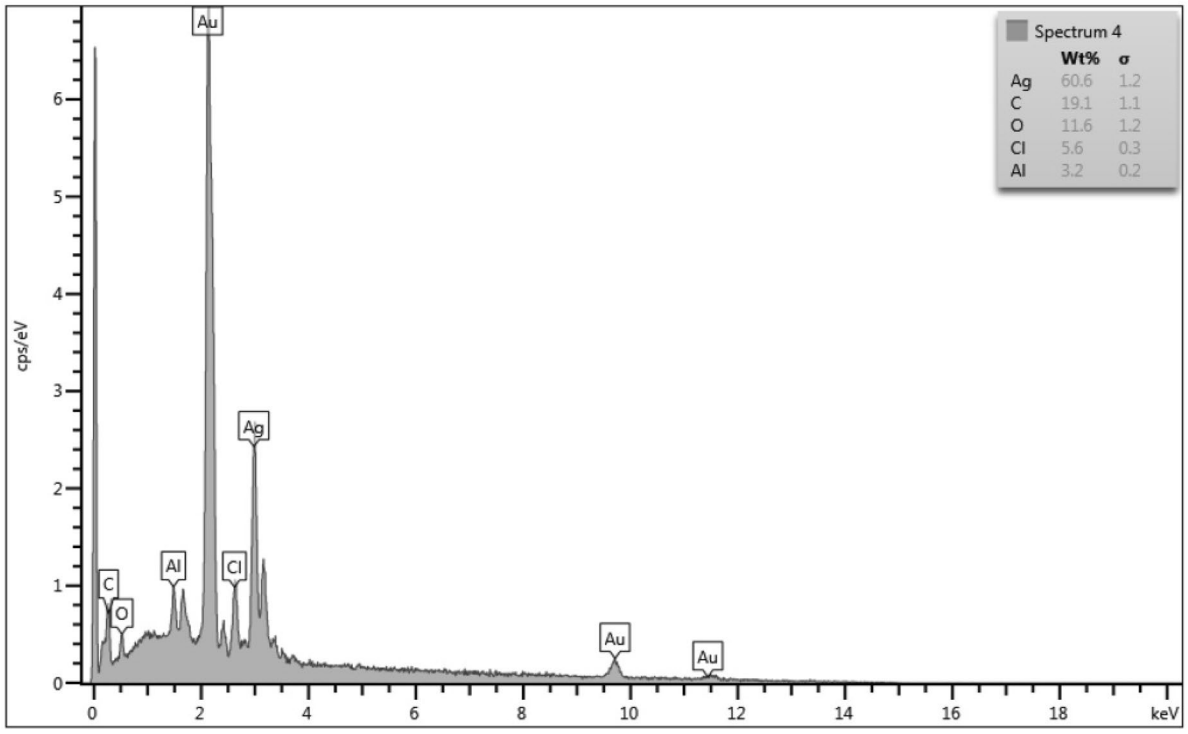

Fig. 8 EDX image of synthesized silver nanoparticles using extract of *Boswellia sacra* leaf

to 37.50 nm (Fig. 9). Similar result was reported with diameter range of 17.9–24.8 nm (Iqbal et al., 2021).

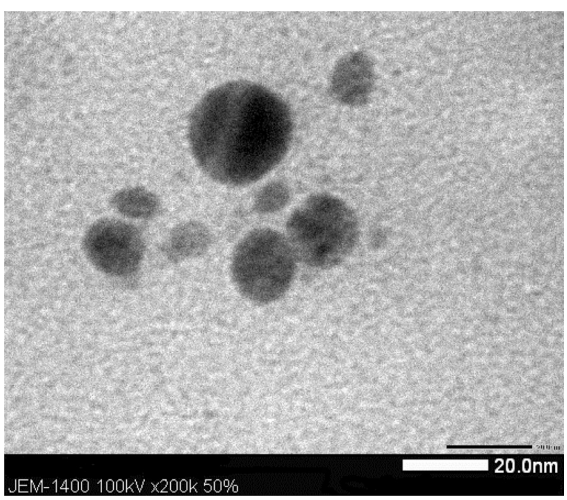

Fig. 9 TEM image of synthesized silver nanoparticles using extract of *Boswellia sacra* leaf (AgNPs diameter size 20 nm; range 11.17–37.50 nm)

Antimicrobial activities

10 mg mL^{-1} of each *Boswellia sacra* leaves extract, $AgNO_3$, silver nanoparticles, and ampicillin as control was applied against *Staphylococcus aureus* (Gram positive) and *Escherichia coli* (Gram negative) using disk diffusion method. The diameter of inhibitory zone was in the range of 24.5 to 10.1 mm (Table 5). The highest inhibitory effect of AgNPs was observed against Gram-positive bacteria (*Staphylococcus aureus)* (Fig. 10).

In case of antifungal activity, literature inhibitory diameter of 10 mg mL^{-1} nystatin as control (Baskaran et al., 2016) was compared with inhibitory diameter of 10 mg mL^{-1} of each *Boswellia sacra* leaves extract, $AgNO_3$, and silver nanoparticles against fungi (*Penicillium chrysogenum* and *Rhizopus oryzae*). The results are summarized in Table 5. The highest inhibitory effect of AgNPs was observed against *Penicillium chrysogenum* (Fig. 10). Silver nanoparticles because of high surface area penetrated well into the cell wall of *Staphylococcus aureus and E. coli* and invaded them. In addition to this,

Table 5 Antimicrobial activity of 10 mg mL^{-1} standard antibiotics, silver nitrate, silver nanoparticles, and *Boswellia sacra* leaf extract against different pathogens

S.No	Microorganisms	1. ampicillin (control)	2. $AgNO_3$	3. AgNPs	4. *B. sacra* leaf extract
	Bacteria	Zone of inhibition (mm)*			
1	*Escherichia coli*	19.5	19.5	20.0	11.1
2	*Staphylococcus aureus*	24.5	19.0	24.0	10.1
	Fungi	Nystatin (Control)	1. *B. sacra* leaf extract	2. $AgNO_3$	3. AgNPs
		Zone of inhibition (mm)*			
1	*Penicillium chrysogenum*	18.8	12.1	11.0	12.9
2	*Rhizopus oryzae*	13.9	11.5	11.0	12.1

*3 determinations were performed ($n = 3$)

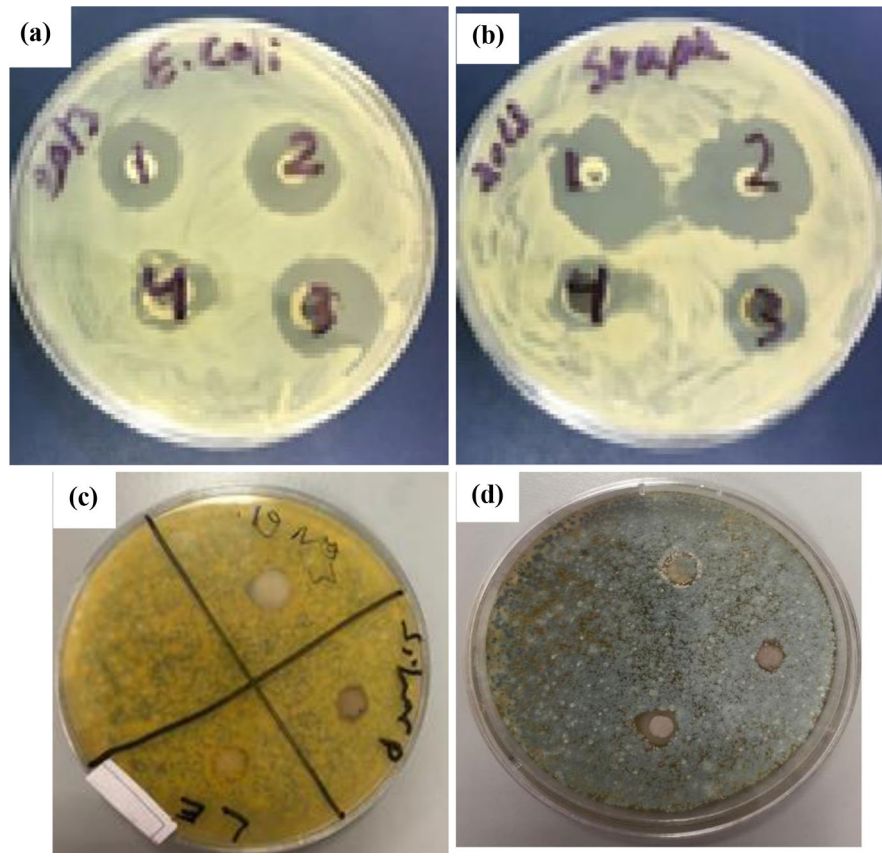

Fig. 10 Antibacterial activity (**a**) *Escherichia coli* and (**b**) *Staphylococcus aureus* and antifungal activities (**c**) *Rhizopus oryzae* and (**d**) *Penicillium chrysogenum*

silver nanoparticles inhibited mycelial growth of *Penicillium chrysogenum* and *Rhizopus oryzae.* The synthesized silver nanoparticles are effective against bacteria and fungi together.

Conclusions

Silver nanoparticles were successfully synthesized using *Boswellia sacra* leaf extract at 55 °C. *Boswellia*

sacra is a commonly available species in Oman. The availability of the plant leaf is easily accessible. The synthesis of silver nanoparticles using *Boswellia sacra* leaf extract was firstly attempted. The synthesis is a simple, safe, clean, economical, reliable, and one-pot synthesis. Synthesized silver nanoparticles were well characterized by UV–visible spectroscopy, FT-IR, SEM, EDS, and XRD techniques. XRD pattern confirmed successful synthesis of silver nanoparticles as face-centered cubic where crystallite sizes of silver nanoparticles were in the range of 11.17 to 37.50 nm. The silver nanoparticles showed antimicrobial activities against bacteria and fungi. AgNPs could be considered as a potential drug delivery carrier.

Acknowledgements The authors (B.M.H. Al-Jassasi, H.M.S. Al-Sawafi, S.H.G. Al-Shukaili) are thankful to the Research Council, Sultanate of Oman, for providing undergraduate research grant (BFP/URG/CBS/19/042) under the supervisorship of S.N.H. Azmi. The authors are grateful to the higher-up and the Vice Chancellor of the University of Technology and Applied Sciences (Higher College of Technology) Muscat, Sultanate of Oman, for support to carry out this work.

Data availability The datasets (crystallite size of AgNPs) generated during the current study are available/confirmed in the name [XRD Crystallite (grain) size calculator (Scherrer equation) using weblink: https://instanano.com/characterization/calculator/xrd/crystallite-size/]. The datasets generated during and/or analyzed during the current study are available from the corresponding author on reasonable request. All data generated or analyzed during this study are included in this published article.

Declarations

Conflict of interest The authors declare no competing interests.

References

Ahmad, S., Munir, S., Zeb, N., et al. (2019). Green nanotechnology: a review on green synthesis of silver nanoparticles — an ecofriendly approach. *International Journal of Nanomedicine, 14*, 5087–5107. https://doi.org/10.2147/IJN.S200254

Ahmed, S., Ahmad, M., Swami, B. L., & Ikram, S. (2016). A review on plants extract mediated synthesis of silver nanoparticles for antimicrobial applications: a green expertise. *Journal of Advanced Research, 7*, 17–28. https://doi.org/10.1016/j.jare.2015.02.007

Al-Harrasi, A., & Al-Saidi, S. (2008). Phytochemical analysis of the essential oil from botanically certified oleogum resin of Boswellia sacra (Omani luban). *Molecules, 13*, 2181–2189. https://doi.org/10.3390/molecules13092181

Al-Harrasi, A., Rehman, N. U., Khan, A. L., et al. (2018). Chemical, molecular and structural studies of boswellia species: B-boswellic aldehyde and 3-epi-11β-dihydroxy ba as precursors in biosynthesis of boswellic acids. *PLoS One, 13,* 1–19. https://doi.org/10.1371/journal.pone.0198666

Alqadi, M. K., Abo Noqtah, O. A., Alzoubi, F. Y., et al. (2014). PH effect on the aggregation of silver nanoparticles synthesized by chemical reduction. *Materials Science - Poland, 32*, 107–111. https://doi.org/10.2478/s13536-013-0166-9

Azmi, S. N. H., Al-Balushi, M., Al-Siyabi, F., et al. (2020). Adsorptive removal of Pb(II) ions from groundwater samples in Oman using carbonized Phoenix dactylifera seed (Date stone). *Journal of King Saud University - Science, 32,* 2931–2938. https://doi.org/10.1016/j.jksus.2020.07.015

Baskaran, X., Vigila, A. V. G., Parimelazhagan, T., Muralidhara-Rao, D., & Zhang, S. (2016). Biosynthesis, characterization, and evaluation of bioactivities of leaf extract-mediated biocompatible silver nanoparticles from an early tracheophyte, Pteris tripartita Sw. *International journal of nanomedicine*, *11*, 5789–5805. https://doi.org/10.2147/IJN.S10820

Chen, S., Drehmel, J. R., & Penn, R. L. (2020). Facile synthesis of monodispersed Ag NPs in ethylene glycol using mixed capping agents. *ACS Omega, 5*, 6069–6073. https://doi.org/10.1021/acsomega.9b04492

De Matteis, V., Malvindi, M. A., Galeone, A., et al. (2015). Negligible particle-specific toxicity mechanism of silver nanoparticles: the role of Ag+ ion release in the cytosol. *Nanomedicine: Nanotechnology, Biology and Medicine, 11,* 731–739. https://doi.org/10.1016/j.nano.2014.11.002

Dong, C., Cao, C., Zhang, X., et al. (2017). Wolfberry fruit (Lycium barbarum) extract mediated novel route for the green synthesis of silver nanoparticles. *Optik (Stuttg), 130,* 162–170. https://doi.org/10.1016/j.ijleo.2016.11.010

Esfanddarani, H. M., Kajani, A. A., & Bordbar, A. K. (2018). Green synthesis of silver nanoparticles using flower extract of Malva sylvestris and investigation of their antibacterial activity. *IET Nanobiotechnology, 12*, 412–416. https://doi.org/10.1049/iet-nbt.2017.0166

Gajendran, B., Durai, P., Varier, K. M., et al. (2019). Green synthesis of silver nanoparticle from Datura inoxia flower extract and its cytotoxic activity. *Bionanoscience, 9*, 564–572. https://doi.org/10.1007/s12668-019-00645-9

Garibo, D., Borbón-Nuñez, H. A., de León, J. N. D., et al. (2020). Green synthesis of silver nanoparticles using Lysiloma acapulcensis exhibit high-antimicrobial activity. *Science and Reports, 10*, 1–11. https://doi.org/10.1038/s41598-020-69606-7

Gole, A., Dash, C., Ramakrishnan, V., et al. (2001). Pepsin-gold colloid conjugates: preparation, characterization, and enzymatic activity. *Langmuir, 17*, 1674–1679. https://doi.org/10.1021/la001164w

Gudikandula, K., & Charya Maringanti, S. (2016). Synthesis of silver nanoparticles by chemical and biological methods and their antimicrobial properties. *Journal of Experimental Nanoscience, 11*, 714–721. https://doi.org/10.1080/17458080.2016.1139196

Gusrizal, G., Santosa, S. J., Kunarti, E. S., Rusdiarso, B. (2017). Synthesis of silver nanoparticles by reduction of silver ion with m-hydroxybenzoic acid. *Asian Journal*

of Chemistry, *29*, 1417–1422. https://doi.org/10.14233/ajchem.2017.20436

Guzman, M., Dille, J., & Godet, S. (2012). Synthesis and antibacterial activity of silver nanoparticles against gram-positive and gram-negative bacteria. *Nanomedicine Nanotechnology, Biology and Medicine, 8,* 37–45. https://doi.org/10.1016/j.nano.2011.05.007

Hamedi, S., & Shojaosadati, S. A. (2019). Rapid and green synthesis of silver nanoparticles using Diospyros lotus extract: evaluation of their biological and catalytic activities. *Polyhedron, 171*, 172–180. https://doi.org/10.1016/j.poly.2019.07.010

Hamidpour, R., Hamidpour, S., Hamidpour, M., & Shahlari, M. (2013). Frankincense (Rŭ Xiāng; Boswellia species): from the selection of traditional applications to the novel phytotherapy for the prevention and treatment of serious diseases. *Journal of Traditional & Complementary Medicine, 3*, 221–226. https://doi.org/10.4103/2225-4110.119723

Hasnain, M. S., Javed, M. N., Alam, M. S., et al. (2019). Purple heart plant leaves extract-mediated silver nanoparticle synthesis: optimization by Box-Behnken design. *Materials Science and Engineering: C, 99,* 1105–1114. https://doi.org/10.1016/j.msec.2019.02.061

Iqbal, N., Iqubal, S. M. S., Khan, A. A., et al. (2021). Effect of CTABr (surfactant) on the kinetics of formation of silver nanoparticles by Amla extract. *Journal of Molecular Liquids*, *329*. https://doi.org/10.1016/j.molliq.2021.115537

Jyoti, K., Baunthiyal, M., & Singh, A. (2016). Characterization of silver nanoparticles synthesized using Urtica dioica Linn. leaves and their synergistic effects with antibiotics. *Journal of Radiation Research and Applied Science, 9*, 217–227. https://doi.org/10.1016/j.jrras.2015.10.002

Kathiravan, V., Ravi, S., & Ashokkumar, S. (2014). Synthesis of silver nanoparticles from Melia dubia leaf extract and their in vitro anticancer activity. *Spectrochimica Acta Part A: Molecular and Biomolecular Spectroscopy, 130,* 116–121. https://doi.org/10.1016/j.saa.2014.03.107

Kimling, J., Maier, M., Okenve, B., et al. (2006). Turkevich method for gold nanoparticle synthesis revisited. *The Journal of Physical Chemistry B, 110*, 15700–15707. https://doi.org/10.1021/jp061667w

Kostoff, R. N., Koytcheff, R. G., & Lau, C. G. Y. (2007). Global nanotechnology research literature overview. *Technological forecasting and social change, 74,* 1733–1747. https://doi.org/10.1016/j.techfore.2007.04.004

Kumar, B., Smita, K., Cumbal, L., & Debut, A. (2017). Green synthesis of silver nanoparticles using Andean blackberry fruit extract. *Saudi Journal of Biological Sciences, 24,* 45–50. https://doi.org/10.1016/j.sjbs.2015.09.006

Küp, F. Ö., Çoşkunçay, S., & Duman, F. (2020). Biosynthesis of silver nanoparticles using leaf extract of Aesculus hippocastanum (horse chestnut): evaluation of their antibacterial, antioxidant and drug release system activities. *Materials Science and Engineering: C, 107*, 110207. https://doi.org/10.1016/j.msec.2019.110207

Martínez-Castañón, G. A., Niño-Martínez, N., Martínez-Gutierrez, F., et al. (2008). Synthesis and antibacterial activity of silver nanoparticles with different sizes. *Journal of Nanoparticle Research, 10,* 1343–1348. https://doi.org/10.1007/s11051-008-9428-6

Masum, M. I., Siddiqa, M. M., Ali, K. A., et al. (2019). Biogenic synthesis of silver nanoparticles using phyllanthus emblicafruit extract and its inhibitory action against the pathogen acidovorax oryzaestrain RS-2 of rice bacterial brown stripe. *Frontiers in Microbiology, 10*, 1–18. https://doi.org/10.3389/fmicb.2019.00820

Moteriya, P., & Chanda, S. (2017). Synthesis and characterization of silver nanoparticles using Caesalpinia pulcherrima flower extract and assessment of their in vitro antimicrobial, antioxidant, cytotoxic, and genotoxic activities. *Artificial cells, nanomedicine, and biotechnology, 45,* 1556–1567. https://doi.org/10.1080/21691401.2016.1261871

Mousavi, S. M., Hashemi, S. A., Ghasemi, Y., et al. (2018). Green synthesis of silver nanoparticles toward bio and medical applications: review study. *Artificial cells, nanomedicine, and biotechnology, 46,* S855–S872. https://doi.org/10.1080/21691401.2018.1517769

National Bureau of Standards Monograph. (1985). Standard x-ray diffraction powder pattern section 21-data for 92 substances, U.S. Department of Commerce, p. 2.

Nikaeen, G., Yousefinejad, S., Rahmdel, S., et al. (2020). Central composite design for optimizing the biosynthesis of silver nanoparticles using plantago major extract and investigating antibacterial, antifungal and antioxidant activity. *Science and Reports, 10*, 1–16. https://doi.org/10.1038/s41598-020-66357-3

Othman, A. M., Elsayed, M. A., Elshafei, A. M., & Hassan, M. M. (2017). Application of response surface methodology to optimize the extracellular fungal mediated nanosilver green synthesis. *Journal of Genetic Engineering & Biotechnology, 15,* 497–504. https://doi.org/10.1016/j.jgeb.2017.08.003

Pastoriza-Santos, I., & Liz-Marzán, L. M. (2002). Synthesis of silver nanoprisms in DMF. *Nano Letters, 2*, 903–905. https://doi.org/10.1021/nl025638i

Pirtarighat, S., Ghannadnia, M., & Baghshahi, S. (2019). Green synthesis of silver nanoparticles using the plant extract of Salvia spinosa grown in vitro and their antibacterial activity assessment. *Journal of Nanostructure in Chemistry, 9,* 1–9. https://doi.org/10.1007/s40097-018-0291-4

Preetha, D., Arun, R., Kumari, P., & Aarti, C. (2013). Synthesis and characterization of silver nanoparticles using cannonball leaves and their cytotoxic activity against Mcf-7 cell line. *Journal of nanotechnology, 2013,* 1–5.

Quintero-Quiroz, C., Acevedo, N., Zapata-Giraldo, J., et al. (2019). Optimization of silver nanoparticle synthesis by chemical reduction and evaluation of its antimicrobial and toxic activity. *Biomaterials research, 23,* 1–15. https://doi.org/10.1186/s40824-019-0173-y

Rafique, M., Sadaf, I., Rafique, M. S., & Tahir, M. B. (2017). A review on green synthesis of silver nanoparticles and their applications. *Artificial cells, nanomedicine, and biotechnology, 45,* 1272–1291. https://doi.org/10.1080/21691401.2016.1241792

Rahman, N., & Nasir, M. (2020a). Facile synthesis of thiosalicylic acid functionalized silica gel for effective removal of Cr(III): Equilibrium modeling, kinetic and thermodynamic studies. *Environ Nanotechnology, Monit Manag, 14*, 100353. https://doi.org/10.1016/j.enmm.2020.100353

Rahman, N., & Nasir, M. (2020b). Effective removal of acetaminophen from aqueous solution using Ca (II)-doped chitosan/β-cyclodextrin composite. *Journal of Molecular*

Liquids, 301, 112454. https://doi.org/10.1016/j.molliq.2020.112454

Rahman, N., Sameen, S., & Kashif, M. (2019). Application of Box-Behnken design and desirability function in the optimization of spectrophotometric method for the quantification of WADA banned drug: Acetazolamide. *Journal of Molecular Liquids, 274*, 270–277. https://doi.org/10.1016/j.molliq.2018.10.120

Rahman, N., & Varshney, P. (2020). Assessment of ampicillin removal efficiency from aqueous solution by polydopamine/zirconium(iv) iodate: optimization by response surface methodology. *RSC Advances, 10*, 20322–20337. https://doi.org/10.1039/d0ra02061c

Rajput, S., Kumar, D., & Agrawal, V. (2020). Green synthesis of silver nanoparticles using Indian Belladonna extract and their potential antioxidant, anti-inflammatory, anticancer and larvicidal activities. *Plant Cell Reports, 39*, 921–939. https://doi.org/10.1007/s00299-020-02539-7

Rautela, A., Rani, J. (2019). Debnath (Das), M. Green synthesis of silver nanoparticles from Tectona grandis seeds extract: characterization and mechanism of antimicrobial action on different microorganisms. *Journal of Analytical Science and Technology*, *10*. https://doi.org/10.1186/s40543-018-0163-z

Raveendran, P., Fu, J., & Wallen, S. L. (2006). A simple and "green" method for the synthesis of Au, Ag, and Au–Ag alloy nanoparticles. *Green Chemistry, 8*, 34–38. https://doi.org/10.1039/b512540e

Riaz, M., Mutreja, V., Sareen, S., et al. (2021). Exceptional antibacterial and cytotoxic potency of monodisperse greener AgNPs prepared under optimized pH and temperature. *Science and Reports, 11*, 1–11. https://doi.org/10.1038/s41598-021-82555-z

Sangaonkar, G. M., & Pawar, K. D. (2018). Garcinia indica mediated biogenic synthesis of silver nanoparticles with antibacterial and antioxidant activities. *Colloids Surfaces B Biointerfaces, 164*, 210–217. https://doi.org/10.1016/j.colsurfb.2018.01.044

Seifipour, R., Nozari, M., & Pishkar, L. (2020). Green synthesis of silver nanoparticles using Tragopogon collinus leaf extract and study of their antibacterial effects. *Journal of Inorganic and Organometallic Polymers and Materials, 30*, 2926–2936. https://doi.org/10.1007/s10904-020-01441-9

Shaik, M. R., Khan, M., Kuniyil, M., et al. (2018). Plant-extract-assisted green synthesis of silver nanoparticles using Origanum vulgare L. extract and their microbicidal activities. *Sustain, 10*, 1–14. https://doi.org/10.3390/su10040913

Song, J. Y., & Kim, B. S. (2009). Rapid biological synthesis of silver nanoparticles using plant leaf extracts. *Bioprocess and Biosystems Engineering, 32*, 79–84. https://doi.org/10.1007/s00449-008-0224-6

Sun, L., Zhang, Z., & Dang, H. (2003). A novel method for preparation of silver nanoparticles. *Materials Letters, 57*, 3874–3879. https://doi.org/10.1016/S0167-577X(03)00232-5

Tarannum, N., & Divya, G. Y. K. (2019). Facile green synthesis and applications of silver nanoparticles: a state-of-the-art review. *RSC Advances, 9*, 34926–34948. https://doi.org/10.1039/c9ra04164h

United States Patent (US 9,795,634 B1). (2017). Moses SL, Drug delivery systems and methods for treating cancer using gold nanoparticles coated with citrate ions, frankincense and myrrh.

Velsankar, K., Preethi, R., Ram, P. S. J., et al. (2020). Evaluations of biosynthesized Ag nanoparticles via Allium Sativum flower extract in biological applications. *Applied Nanoscience, 10*, 3675–3691. https://doi.org/10.1007/s13204-020-01463-2

Xu, L., Wang, Y. Y., Huang, J., et al. (2020). Silver nanoparticles: synthesis, medical applications and biosafety. *Theranostics, 10*, 8996–9031. https://doi.org/10.7150/thno.45413

Yousaf, H., Mehmood, A., Ahmad, K. S., & Raffi, M. (2020). Green synthesis of silver nanoparticles and their applications as an alternative antibacterial and antioxidant agents. *Materials Science and Engineering C, 112*, 110901. https://doi.org/10.1016/j.msec.2020.110901

Zhang, Q., Li, N., Goebl, J., et al. (2011). A systematic study of the synthesis of silver nanoplates: is citrate a "magic" reagent? *Journal of the American Chemical Society, 133*, 18931–18939. https://doi.org/10.1021/ja2080345

Zhang, Z., Shen, W., Xue, J., et al. (2018). Recent advances in synthetic methods and applications of silver nanostructures. *Nanoscale Research Letters*, *13*. https://doi.org/10.1186/s11671-018-2450-4